Space-time spectral element methods for unsteady convection-diffusion problems

Pinhas Z. Bar-Yoseph
Computational Mechanics Laboratory (CML), Faculty of Mechanical Engineering, Technion, Haifa, Israel, and
Eduard Moses
Research and Development Division, Israel Electrical Corporation, Haifa, Israel

Introduction

Let us consider the following system of M partial differential equations[1,2]

$$u_{,t} + {}^{c}f_{i,i} = {}^{d}f_{i,i} + q \qquad in\ G \tag{1}$$

where $u \in \Re^M$ is the solution vector; ${}^{c}f_i \in \Re^M$ is the convective flux vector and ${}^{d}f_i \in \Re^M$ is the diffusive flux vector; q denotes the volume source vector; t is time; comma denotes partial derivative with respect to x_i and the summation convention is used throughout; $\Omega(t)$ is a bounded region in $\Re^{n_{sd}}$ with a piecewise smooth boundary $\Gamma(t)$, where n_{sd} denotes the number of space dimension; $G = \Omega(t) \times I$ denotes the space-time domain with boundary $S = \Gamma(t) \times I$; $I = (0, T)$ is the time interval (T is the final time).

The initial/boundary value problem of (1) consists of finding a function u which satisfies (1), the initial condition $u(x, 0) = u^0(x)$ on $\Omega(0)$ and appropriate well posed boundary conditions of Dirichlet and Neumann type on $S_u = \Gamma_u(t) \times I$ and $S_f = \Gamma_f(t) \times I$ respectively.

The solution method chosen in this work is the spectral element method which was first introduced by Patera[3]. This is a high-order weighted residuals method which exploits the rapid convergence rates of spectral methods while retaining the geometric flexibility of the low-order isoparametric finite element methods. According to the semi-discrete finite element approach, the spatial domain is broken up into macro spectral elements. Within each element, the dependent variables are expanded in terms of pth order tensor product Lagrangian interpolants through the Legendre-Gauss-Lobatto collocation points. The Legendre-Gauss-Lobatto points are clustered near elemental boundaries and are chosen because of their interpolation and quadrature properties.

This research was supported in part by the fund for promotion of research at the Technion.

International Journal of Numerical Methods for Heat & Fluid Flow
Vol. 7 No. 2/3, 1997, pp. 215-235.

Semi-discrete spectral element algorithms for solving equation (1) have been developed for the simulation of unsteady incompressible fluid flow and heat transfer[4]. This semi-discrete approach is of high-order accuracy in space but only of low-order accuracy in time[4,5] and, therefore, the error of the fully discretized method is dominated by the temporal error. This leads naturally to the study of an important class of space-time spectral element methods, allowing balanced accuracy in both space and time directions.

The concept of applying space-time finite element approximations was pioneered in the late 1960s and since then has been expanded and further developed through discontinuous spatial and temporal discretizations[6-19, and references therein].

The purpose of the present work is to investigate the potential of these methods by developing appropriate schemes on a number of selected initial/boundary-value problems and presenting their convergence and stability properties.

The outline of the paper is as follows: first, a computational model is presented, followed by numerical results of various model problems with a discussion. Finally, some conclusions are drawn.

Method of solution

The time interval is partitioned into subintervals $I^n = (t^n, t^{n+1})$ where t^n and t^{n+1} belong to an ordered partition of time levels $0 = t^0 < t^1 < \ldots < t^N = T$. A space-time strip, for the nth time subinterval, is then defined as $G^n = \Omega^n \times I^n$ with boundary $S^n = \Gamma^n \times I^n$ (Figure 1). This strip is then discretized into $(n_{el})^n$ elements, ${}_eG^n = {}_e\Omega^n \times I^n$, $e = 1, 2, \ldots, (n_{el})^n$. Within each element, the dependent variables are expanded in terms of the pth-order tensor product Lagrangian interpolants through the Legendre-Gauss-Lobatto integration points. Applying the Galerkin method to equation (1) in conjunction with the group finite element approximation for the non-linear convection term[1] yields (for each time step) a set of non-linear algebraic equations coupling the nodal unknowns belonging to the same time step. This fully implicit approach (FISTSE) seems less efficient than classical semi-discrete techniques.

In order to increase computational efficiency, the following strategy was suggested[9,19]:

- The non-linear set of equations, including all time sublevels in the solution domain, are solved directly (i.e. using the FISTSE approach) for the first time step only. Afterwards, a time increment ($\Delta\tau$) is chosen such that there is an overlapping time region between the first domain of the solution and the second one (Figure 2). This overlapping includes up to $(p-1)$ time sublevels ($\Delta\tau < T^n$). The approximate solution within the first domain is used to predict the approximate solution within the second domain for the overlapping time sublevels. This is done by applying a projection operator from the first domain to the second one, which can be of the general weighted form (e.g. L_2 projection[20]). This general

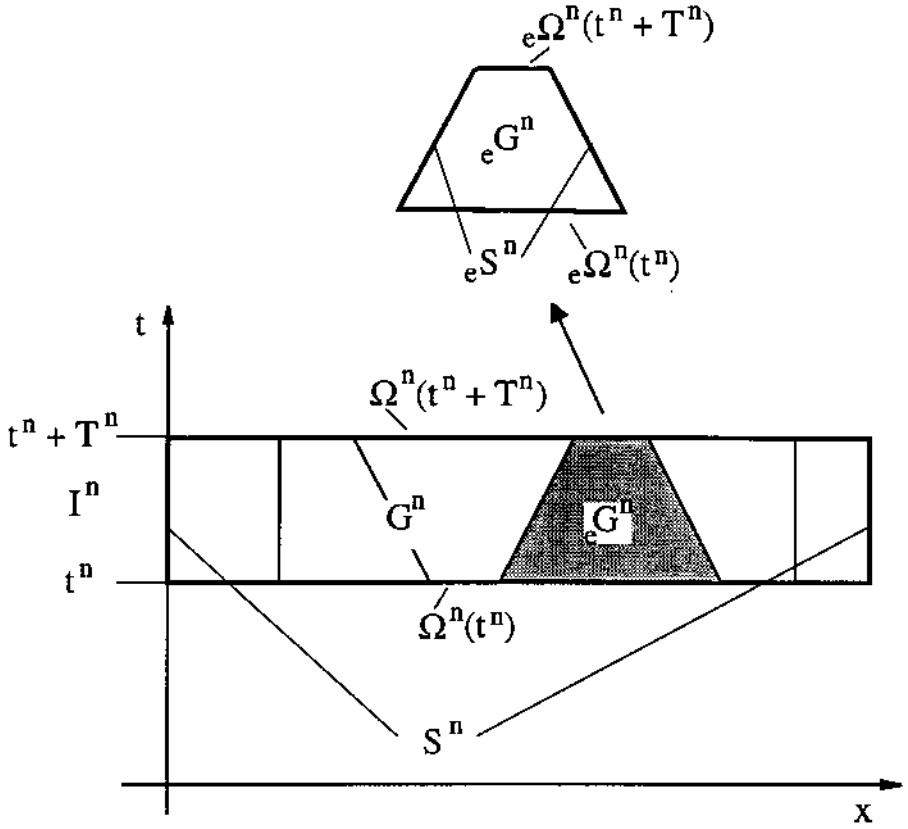

Figure 1.
A space-time strip and its finite element assembly

weighted form may improve performance and be worth investigating. However, in this study our attention is restricted to the simple direct interpolation case[9,19] in order to improve computational efficiency.

The solution of the remaining upper time sublevels belonging to the second domain is then obtained from the set of equations of the discontinuous Galerkin spectral element formulation.

- The coefficient matrix of the approximate solution is partitioned into submatrices so that each submatrix located off-diagonal is a diagonal matrix, while those which are located on the diagonal are full matrices[7,9,19]. This particular structure is used for constructing explicit/implicit algorithms to solve the unknowns located on the upper non-overlapping time sublevels.

The following two space-time spectral element methods were applied to solve equation (1):

(1) *Coupled methods*
- Hyperbolic-dominated equations are treated explicitly (ESTSE).

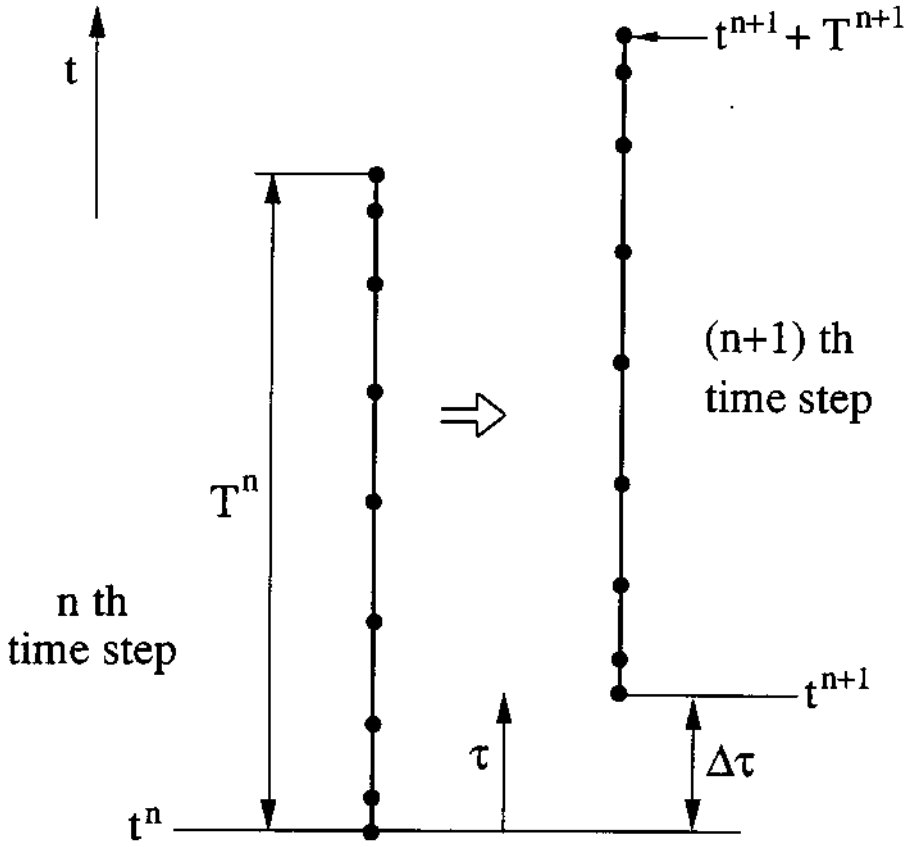

Figure 2.
Schematic illustration of the timewise translation of a mesh consisting of two time elements of degree 8 (the horizontal displacement is not physical but for purposes of visualization

- Parabolic-dominated equations are treated implicitly (ISTSE).

(2) *Splitting methods*

- The first fractional substep uses an explicit or a locally implicit (at the element level) scheme to march the non-linear advection term. In the second fractional substep, the viscous correction is carried out via an implicit scheme (EISTSE).
- The convective term is treated explicitly using *p*th-order Adams-Bashforth multistep schemes. In the second substep, the viscous term is treated implicitly using the above-mentioned space-time spectral element approach (EIABSTSE).

A subcycling technique, in which several hyperbolic substeps are taken for each implicit parabolic substep, was also investigated (CEISTSE).

Splitting techniques may be advantageous if the hyperbolic subproblem is stiff relative to the parabolic one[5] (e.g. when shocks are formed). In this case, the temporal decoupling (with subcycling) is desirable in order to avoid

unnecessary solution of the parabolic subproblem. However, the number of subcycles should be kept low in order to avoid significant loss of accuracy[9].

In this presentation, our primary objectives are to construct the following two substeps weak formulation (STDSE) and to investigate its stability and accuracy.

The hyperbolic substep

The space-time discontinuous Galerkin method is employed as the basis for this formulation which can be written as follows[6].

Within each space-time element ${}_eG^m$, find $\overset{*}{U} \in \overset{*}{\mathsf{U}}$ such that

$$\begin{aligned}
&\int_{eG^m} \left\{ -\overset{*}{W}_{,t} \cdot \overset{*}{U} - \overset{*}{W}_{,i} \cdot^{c} \overset{*}{F}_i \right\} dG + \\
&\int_{e\Omega^m} \left\{ {}^{-}\overset{*}{W}(t^m + T^m) \cdot^{-} \overset{*}{U}(t^m + T^m) - {}^{+}\overset{*}{W}(t^m) \cdot^{+} \overset{*}{U}(t^m) \right\} d\Omega + \\
&\int_{e\Omega^m} {}^{+}\overset{*}{W}(t^m) \cdot [[\overset{*}{U}(t^m)]] d\Omega + \int_{eS^m} {}^{+}\overset{*}{W} \cdot [[{}^{c}\overset{*}{F}_i]] n_i dS + \\
&\int_{eS^m} \overset{*}{W} \cdot^{c} \overset{*}{F}_i n_i dS = \int_{eG^m} \overset{*}{W} \cdot \overset{*}{Q}\, dG; \qquad e = 1, 2, \ldots, (n_{el})^m \\
&\qquad\qquad \forall \overset{*}{W} \in \overset{*}{\mathsf{W}}
\end{aligned} \tag{2}$$

where n is a unit outward normal vector to S; ${}^{\pm}U = \lim_{\varepsilon \to 0} U(\xi \pm \varepsilon)$; the double bracket denotes the jump operator $[[U]] = {}^{+}U - {}^{-}U$ acting on U at ξ located at the inter-element "singular" surfaces. As will be seen in the stability analysis (see also [6-8]), these jump terms are stabilizing operators; $\overset{*}{\mathsf{U}}$ is the space of piecewise polynomials with no continuity requirement across inter-element boundaries and $\overset{*}{\mathsf{W}}$ is the corresponding space of test functions.

Equation (2) defines an algorithm in which the calculations may be performed on an element-by-element basis[6,7]. Consequently, CPU time and storage are not influenced by the nodal numbering. This advantage increases in non-linear applications where frequent refactorizations are typically necessary[6,7]. The initial computing domain is represented by a collection of space-time macro elements. Each of the macro elements may be refined by *h*-, *p*- or *hp*-refinements[6,7]. Switching function representation is a very useful data structure and can be employed efficiently for adaptively generating and refining the mesh[21]. Flux vector splitting with an alternating sweep in the forward and backward space directions has been employed in [6,7]. According to this algorithm, the discontinuities of the split fluxes are weighted along all inter-element boundaries, which results in a physically meaningful upwinding effect. Other numerical flux splitting may improve performance and be worth investigating. The elements near the sharp front can be tilted in such a way that they are aligned with the shock line[7]. Thus, the generalized jump conditions at the singular surfaces can be approximated accurately.

The parabolic substep

The space continuous-time discontinuous Galerkin method is employed as the basis for this formulation which can be written as follows[15,16].

Within each space-time strip G^n, find $U \in \mathsf{U}$ such that

$$\begin{aligned}
&\int_{G^n} \left\{ -W_{,t} \cdot U \; + \; W_{,i} \cdot^{d} F_i \right\} dG \;\; + \\
&\int_{\Omega^n} \left\{ {}^{-}W(t^n \; + \; T^n) \cdot^{-} U(t^n \; + \; T^n) {}^{+}W(t^n) \cdot^{+} U(t^n) \right\} d\Omega \;\; + \\
&\int_{\Omega^n} \; {}^{+}W(t^n) \cdot [[U(t^n)]] d\Omega \;\; - \\
&\int_{S^n} W \cdot^{d} F_i n_i dS \; = \; \int_{G^n} W \cdot \overset{*}{Q} \, dG; \qquad \forall W \in \mathcal{W}
\end{aligned} \tag{3}$$

where for the subcycling approach $m \neq n$; U is the space of piecewise polynomials with no continuity requirement across Ω^n and W is the corresponding space of test functions; $\overset{*}{Q}$ includes the contribution of the convective term calculated at the hyperbolic substep.

Equation (3) defines an algorithm in which the calculations may be performed on one space-time strip at a time. At the end of each time step, a new spatial spectral element mesh can be constructed adaptively according to the distribution of a proper error indicator. This may yield approximations that take advantage more fully of the ideas behind space-time discretizations. This dynamic gridding may also provide significantly improved computational efficiencies by allocating the majority of nodes to the region of the solution domain where they are most needed (e.g. at the inner and outer layers) while using relatively few in regions where the solution has low gradients. For non-linear problems, the solution is being built up iteratively while the mesh is being refined.

Results

The discussion is restricted to selected representative model problems (for more details see [6-9,17-18,22-24]) using the Bubnov-Galerkin method and employing rectangular elements. Equation (1) describes the mass, momentum and energy balance in a one-dimensional flow with heat transfer. By appropriate choice of various terms in this equation, different physical problems can be modelled, e.g. the one-dimensional heat conduction equation (problem 1), the energy equation for a fluid flow of known and constant velocity (problem 2) and the momentum balance equation in a flow with negligible or no pressure gradients (problem 3). These particular problems are useful for purposes of comparison, performance and error evaluation, as they have known analytical solutions.

Problem 1: transient diffusion

$$
\begin{aligned}
{}^{c}f &= 0 \quad ; \quad u(x,0) = u^{0}(x) \\
{}^{d}f &= \frac{\partial u}{\partial x} \; ; \quad u(0,t) = g_1(t) \\
q &= 0 \quad ; \quad u(1,t) = g_2(t)
\end{aligned}
\tag{4}
$$

with the initial and boundary conditions specified so that the exact solution is given by $u = e^{-\pi 2t} \cos(\pi x)$. For the continuous Galerkin method (using the ISTSE approach), the global discrete L_2 error is shown in Figure 3. The slope of the lines indicates that the order of the method is sub-optimal ($||e|| \sim O((\Delta t)^p)$). For $p = 2$, the coupled methods give equations that can be interpreted in terms of finite difference approximations. The ESTSE yields the Richardson explicit approximation which is of second order but is unconditionally unstable and therefore has no practical value. The ISTSE gives a second-order backward difference for the time derivative and central differencing for the space derivative. The stability analysis (based on the matrix method) shows that ISTSE is an unconditionally stable scheme for $2 \leq p \leq 10$. The results corresponding to the time discontinuous Galerkin method (equation 3), are depicted in Figure 4 (n_{dof} denotes the number of degrees of freedom). It is shown that for this formulation the optimal rate of convergence is achieved ($m \sim (p + 1)$). For comparison, the consumed CPU time (on a Dec 5000/200 workstation) is also shown.

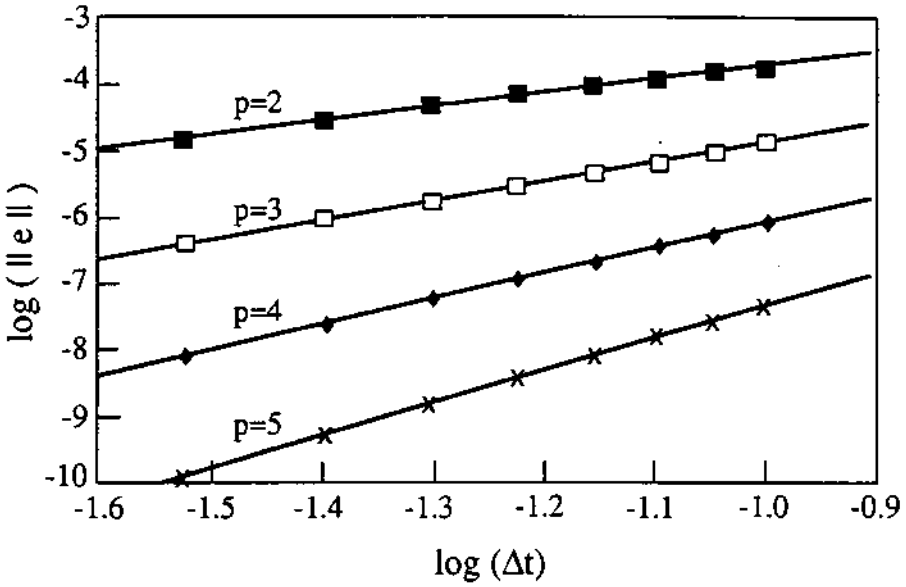

Figure 3. Problem 1 – Convergence rates and CPU time for various polynominal degrees (ISTSE)

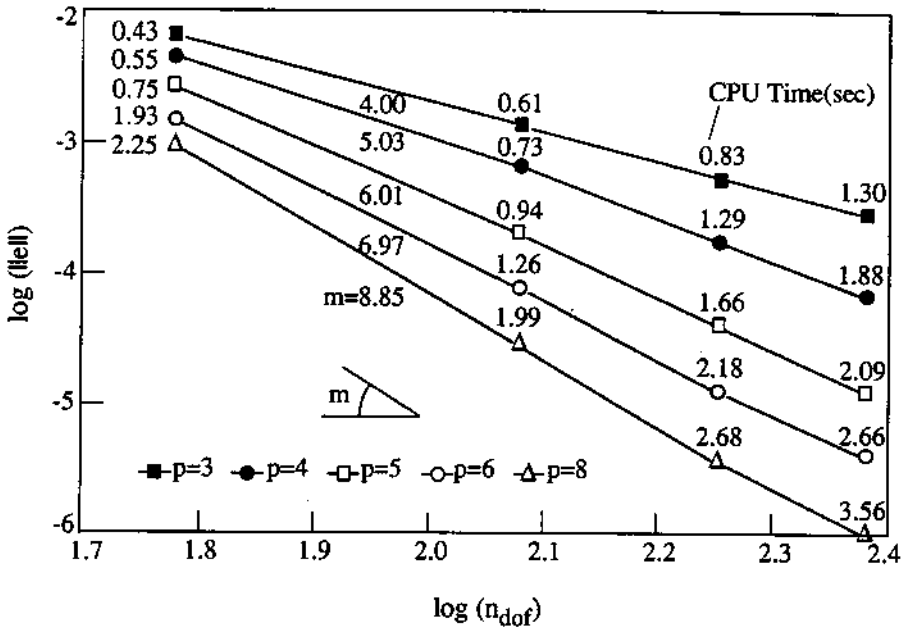

Figure 4.
Problem 1 – Convergence rates and CPU time for various polynomial degrees (STDSE)

Problem 2: transient linear convection-diffusion

$$\begin{aligned} {}^{c}f &= V\,u \;\; ; \quad u(x,0) = u^0(x) \\ {}^{d}f &= \nu\frac{\partial u}{\partial x} \; ; \quad u(0,t) = g_1(t) \\ q &= 0 \quad\;\; ; \quad u(l,t) = g_2(t) \end{aligned} \tag{5}$$

where V is taken to be constant. This linear problem is employed both for a priori (Fourier-based) as well as a posteriori stability and accuracy analyses. The initial conditions consist of the Gaussian distribution[10,25], i.e. $u^0(x) = \exp\frac{(x-x_0)^2}{2\sigma_0^2}$, $g_1 = 0$, $g_2 = 0$), Adaptive mesh refinement strategies are also analysed.

Fourier analysis conducted for $3 \leq p \leq 5$ showed that the STDSE is unconditionally stable for the whole range of Courant and Fourier numbers. This is to be expected since for each substep the corresponding scheme is unconditionally stable (see [6-8] for the pure hyperbolic case and the previous example for the pure parabolic case).

The Gaussian distribution problem was solved both with a dynamic grid chosen in a heuristic way suggested in [25] and with an adaptive mesh built according to solution gradients. The dynamic grid was built in the following way: the initial mesh consists of three sub-meshes; two of the sub-meshes are located outside the Gaussian bell while the third sub-mesh is located inside it (each of them is uniformly distributed within each sub-region). Afterwards, the central sub-mesh moves with the Gaussian bell group velocity. The propagation

of the Gaussian wave for l = 10, V = 1.0, initial centre of mass x_0 = 3.0, standard deviation σ_0 = 0.3 and v = 0.3 is depicted in Figure 5(a). Figures 5(b) and 5(c) show the solution obtained by using an adaptive grid strategy and a dynamic grid strategy, respectively, as well as the evolution of the grids during the solution progress. The convergence rate has been verified by solving this problem analytically. Figure 6 shows the L_2 error versus the number of degrees of freedom, in the case of the dynamic grid and for different values of the polynomial degree (p = 3, 4, 5, 6, 8). The slope of the lines, m, clearly indicates that the order of the method is (p + 1).

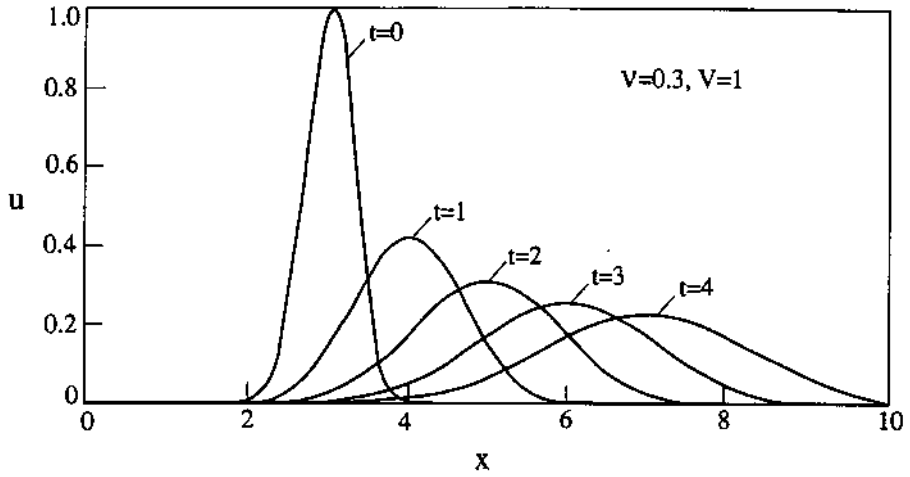

Figure 5a. Problem 2 – Analytic solution for the propagation of a Gaussian wave

Problem 3: transient non-linear convection dominated

Burger's equation is a very suitable model for testing various computational algorithms for convection-dominated flows where severe gradients are created. During the past few years, a great deal of effort has been placed in attempting to compute efficiently the solution of this equation for very small values of the viscosity. Among the computational methods, finite difference, spectral, spectral element and space-time finite element methods have been mainly used[1,7,9,26,27]. Results are presented for the following problem:

$$\begin{aligned} {}^{c}f &= \frac{u^2}{2} \quad ; \quad u(x,0) = -x \\ {}^{d}f &= \nu \frac{\partial u}{\partial x} \; ; \quad u(-1,t) = 0 \\ q &= 0 \quad ; \quad u(1,t) = 0 \end{aligned} \tag{6}$$

The linear stability analysis can be performed only for linear PDEs. Non-linear PDEs must therefore be locally linearized, after which a stability analysis is performed on the local amplification matrix of the corresponding spectral

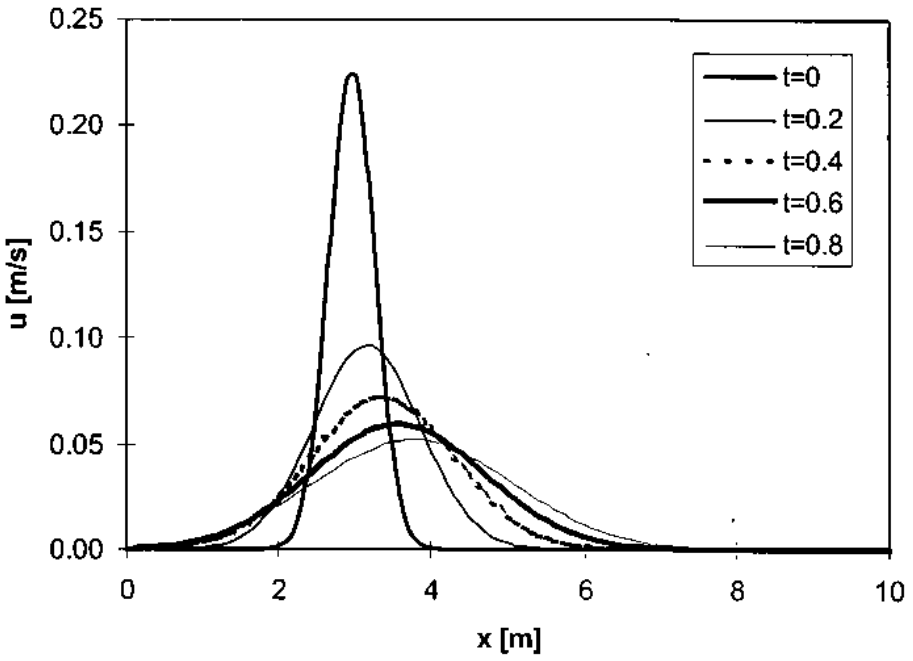

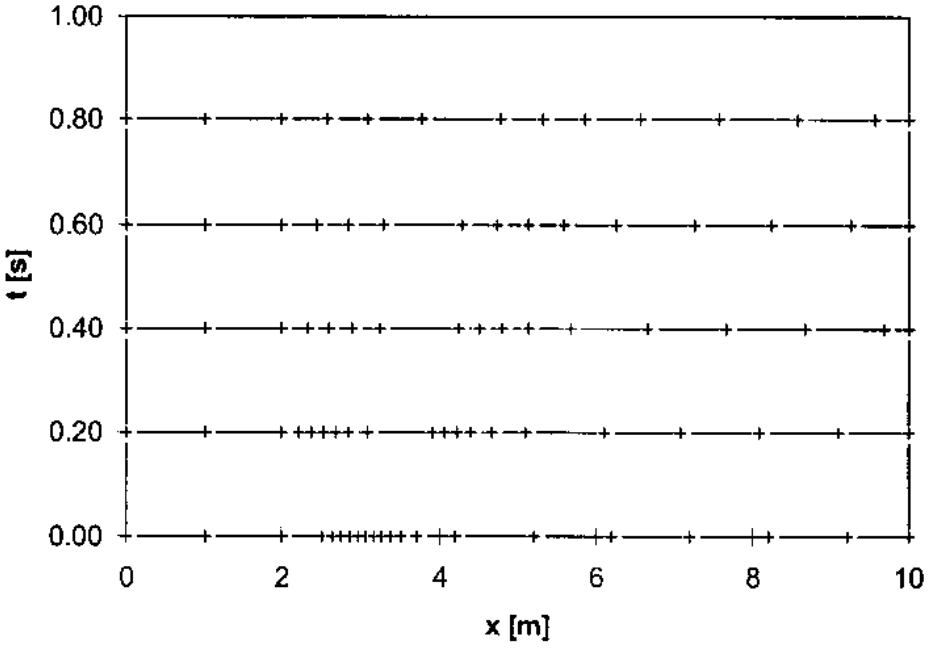

Figure 5b.
Problem 2 – Adaptive mesh solution and the corresponding grids (STDSE)

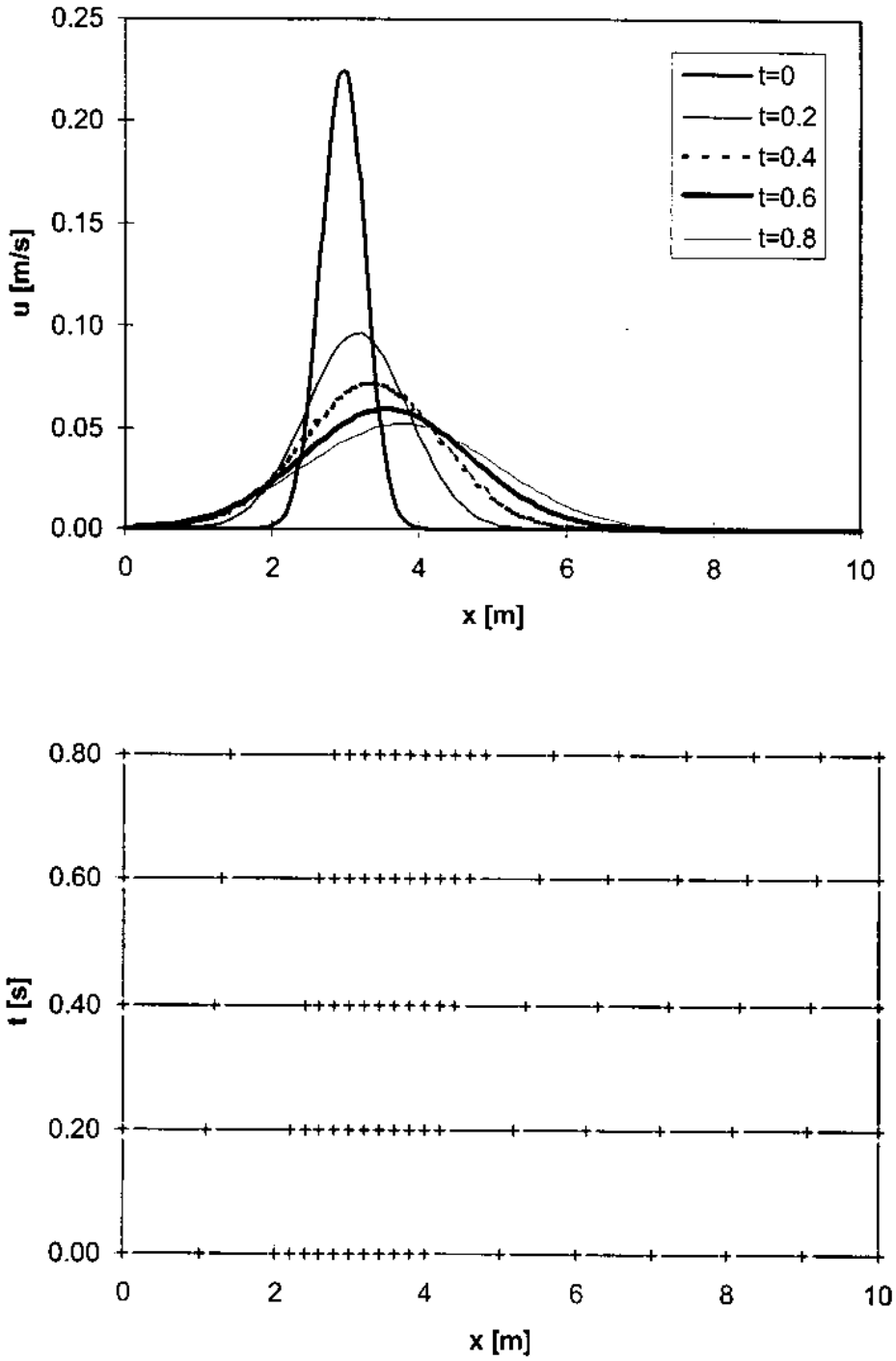

Figure 5c. Problem 2 – Dynamic mesh solution and the corresponding grids (STDSE)

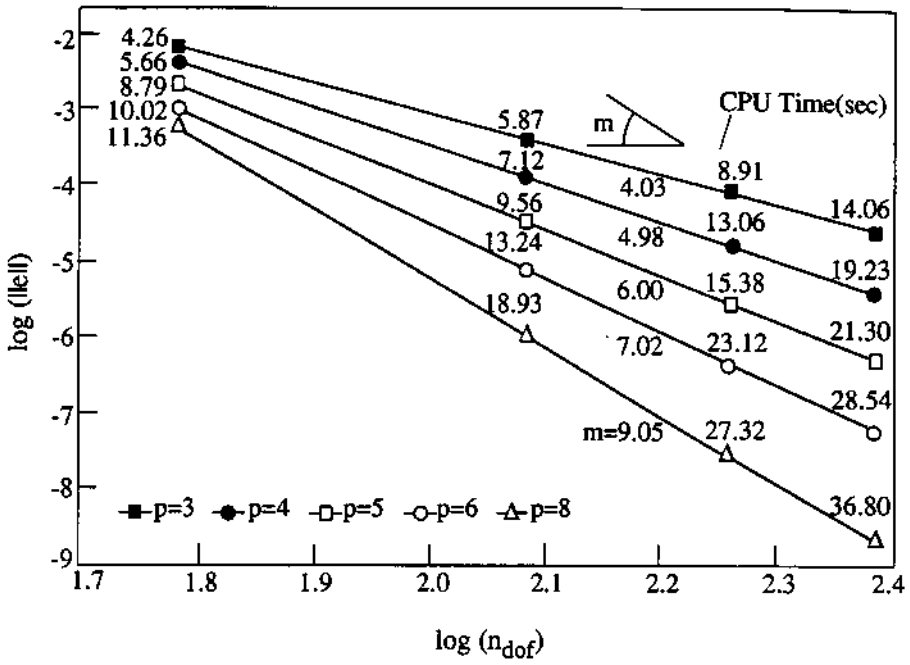

Figure 6.
Problem 2 – Convergence rates and CPU time for the Gaussian Bell initial condition problem and various polynomial degrees (STDSE)

element scheme which approximates the linearized PDEs. The corresponding amplification matrix is time-dependent. Applying this approach results in highlighting some limitations on the mesh parameters (i.e. the Courant and Fourier numbers[9] in the present case).

Figure 7 shows these stability-induced limitations in the form of a Fourier-Courant numbers relationship for both ESTSE[9] and the present discontinuous Galerkin (STDSE) approaches. The schemes are stable for Fourier-Courant number pairs between the respective curves and the horizontal axis. Subsequent numerical experiments show this analysis to be accurate.

Figure 8 shows the CPU time consumption (on a Dec 3000/600 workstation) versus the polynomial degree for two constant error tolerances ($||e|| = \varepsilon$, where $\varepsilon = 1.0 \times 10^{-4}$, 1.0×10^{-5} is measured by the discrete L_2 norm) for both the continuous and discontinuous Galerkin methods.

Figure 9 depicts the influence of subcycling on accuracy and CPU time requirements (on a Dec 3000/600 workstation) for a constant number of degrees of freedom ($n_{dof} = 240$) and for the continuous (CEISTSE[9]) as well as the present discontinuous Galerkin (CSTDSE) methods. It is observed that a few subcycling substeps can yield a small loss of the accuracy while giving a significant reduction in the CPU time.

Convergence analysis was conducted in order to compare the performance of the present formulation (STDSE) with other methods[9]. The error was measured by both the discrete L_2 and H^1 norms. The full rate of convergence is achieved when the error is measured in regions where the solution is

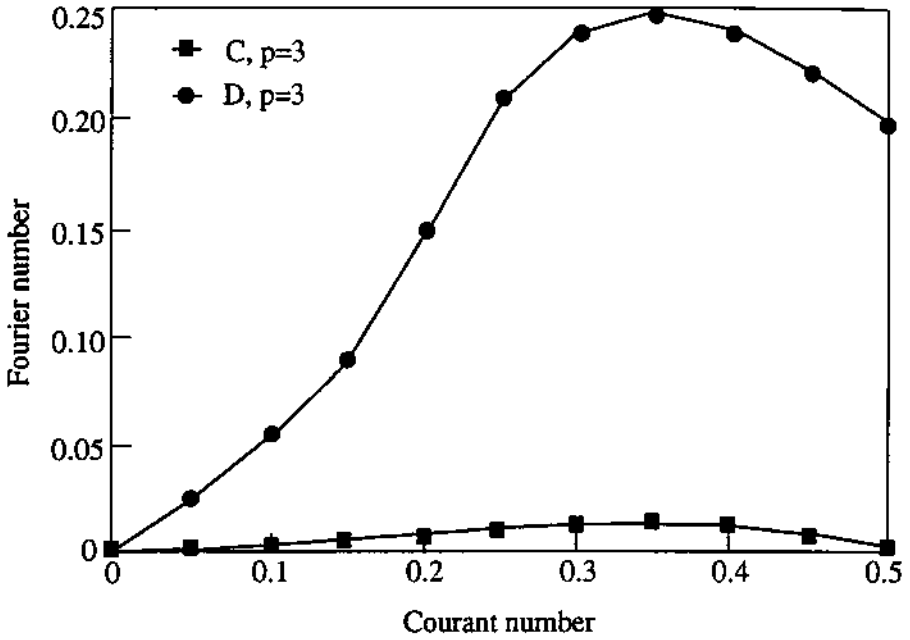

Figure 7. Problem 3 – Locally linearized stability regions (C–ESTSE; D–STDSE). Schemes are stable for Fo-Co pairs between the respective curves and the horizontal axis

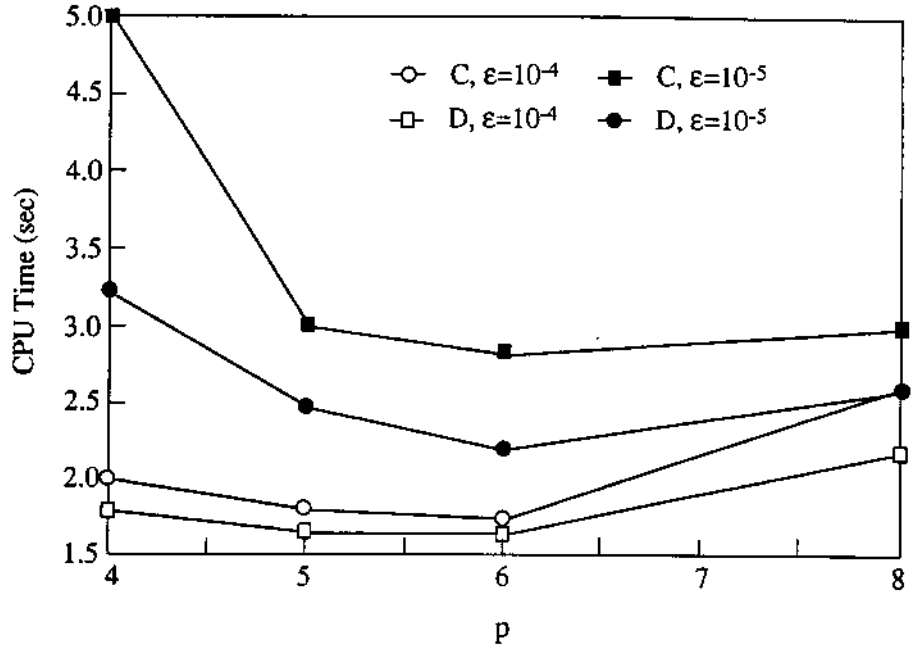

Figure 8. Problem 3 – CPU time consumption (C–ESTSE; D–STDSE)

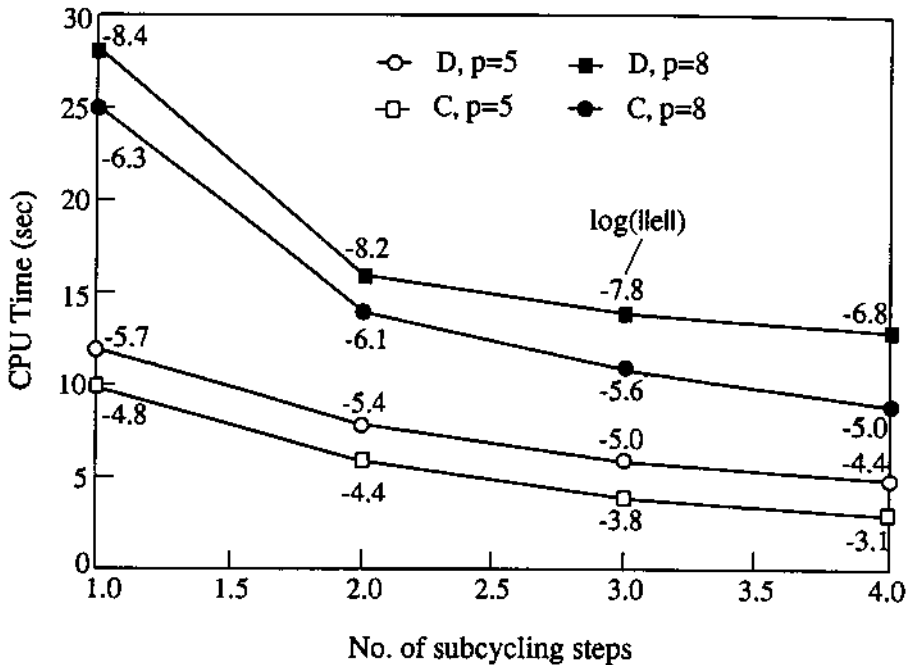

Figure 9.
Problem 3 – CPU time consumption versus number of subcycles (C–CEISTSE; D–CSTDSE)

smooth[7,9]. However, when the shock is included, the rate of convergence (for uniform mesh refinements) is independent of p (it is actually controlled by the "smoothness parameter" of the true solution[7,9,14]).

The effect of p-refinement (p = 2, 4, 6, 8; uniform mesh with the natural clustering of the Legendre-Gauss-Lobatto points; n_{el} = 30, t = 0.1 seconds after the shock wave has been formed); as well as the effect of geometric mesh refinement (q^{-1} is the common factor of the geometric progression; p = 2, n_{el} = 40), on the spurious dispersion are clearly demonstrated in Figures 10 and 11 respectively (for the EISTSE method with $\nu = 1.0 \times 10^{-3}$).

The spurious oscillations can be suppressed efficiently by an adaptive hp–refinement[7,27] or by switching from a time-continuous to a time-discontinuous scheme (the discontinuous jump tends to act as a stabilizer). Figures 12 and 13 show the performance of the continuous and discontinuous space-time spectral elements (ESTSE and STDSE) respectively (on identical uniform grids). It is clearly seen that the STDSE scheme is superior in its shock-capturing features, i.e. suppressing the wiggles and reproducing crisp wave fronts.

Concluding remarks

The main conclusions of this study are as follows:

- The proposed discontinuous spectral element method has been shown to be a computationally efficient scheme for the whole range of physical

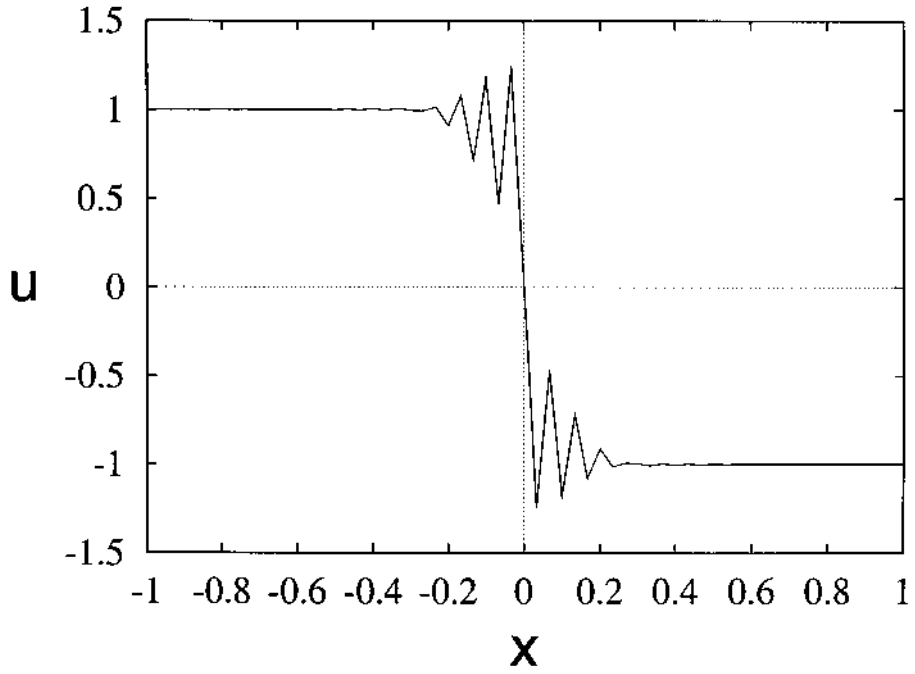

Figure 10(a). Problem 3 – Artificial oscilliations adjacent to the shock front for various p (EISTSE) $p = 2$

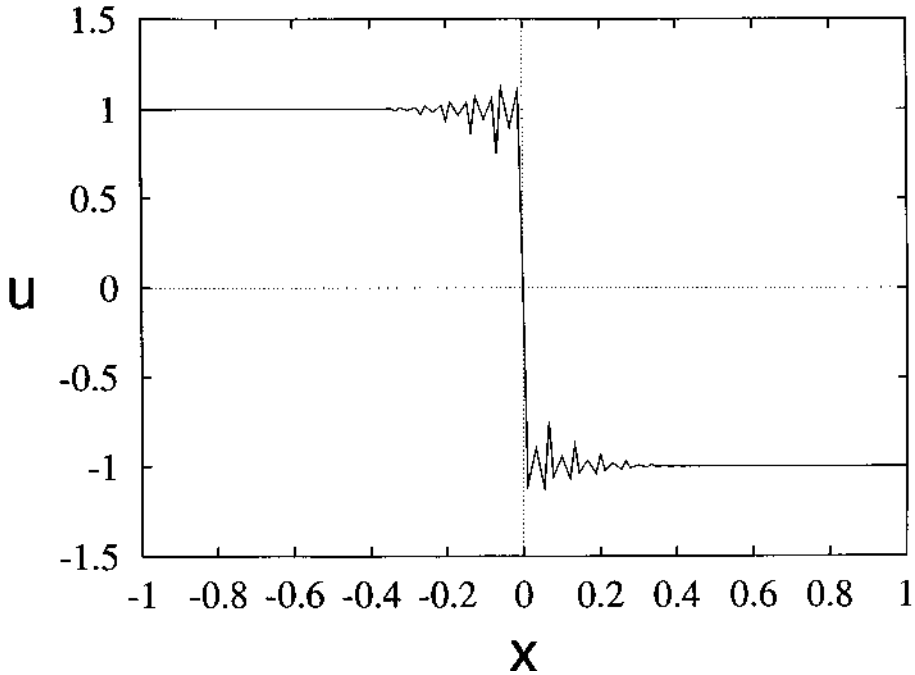

Figure 10(b). Problem 3 – Artificial oscilliations adjacent to the shock front for various p (EISTSE) $p = 4$

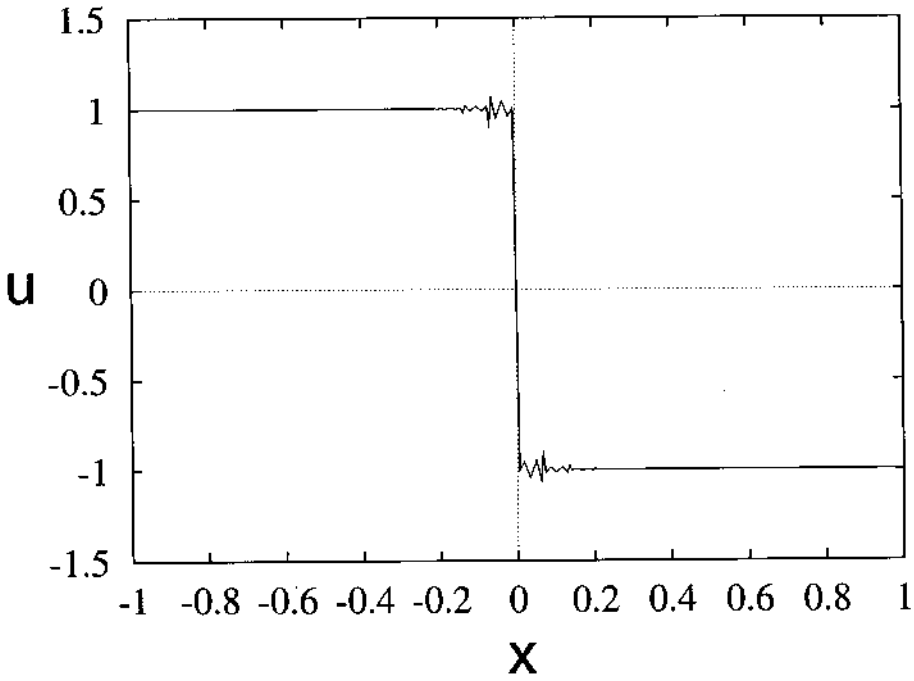

Figure 10(c).
Problem 3 – Artificial oscilliations adjacent to the shock front for various p (EISTSE) $p = 6$

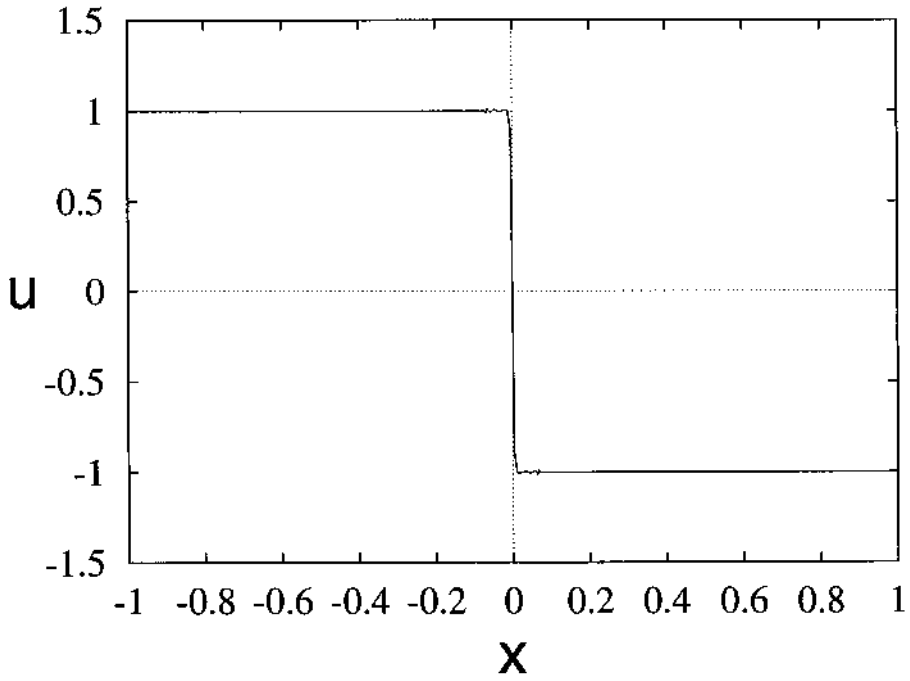

Figure 10(d).
Problem 3 – Artificial oscilliations adjacent to the shock front for various p (EISTSE) $p = 8$

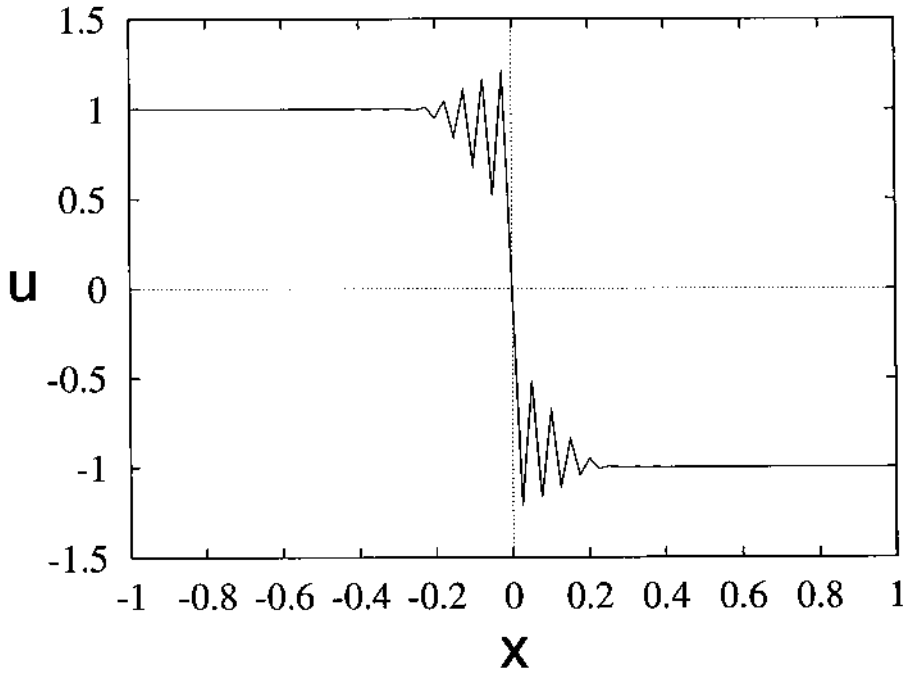

Figure 11(a). Problem 3 – Artificial oscillations adjacent to the shock front for various geometric mesh refinement (EISTSE) $q = 1$ (uniform grid)

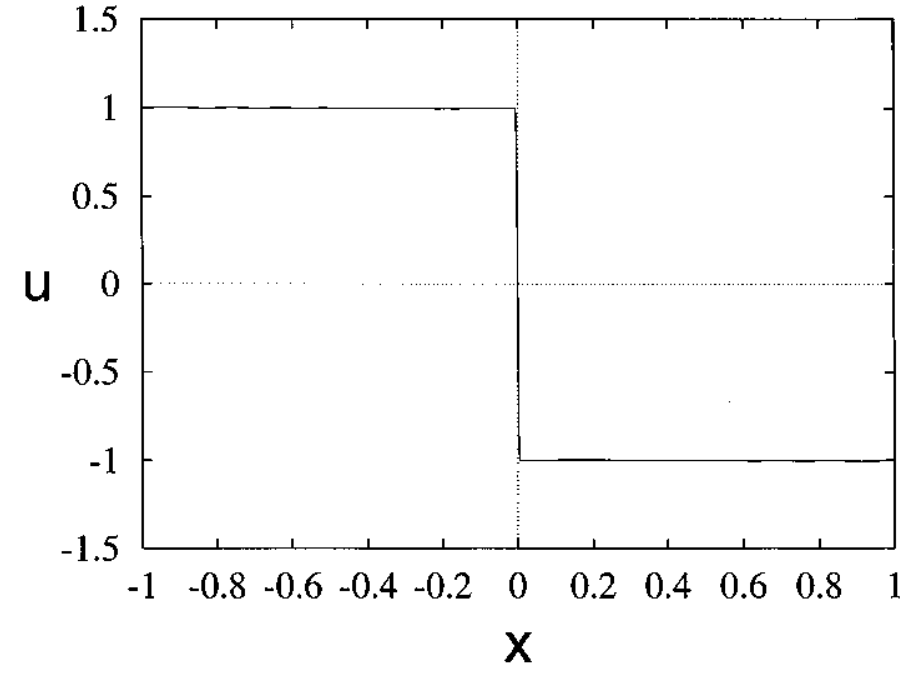

Figure 11(b). Problem 3 – Artificial oscillations adjacent to the shock front for various geometric mesh refinement (EISTSE) $q = 1.2$

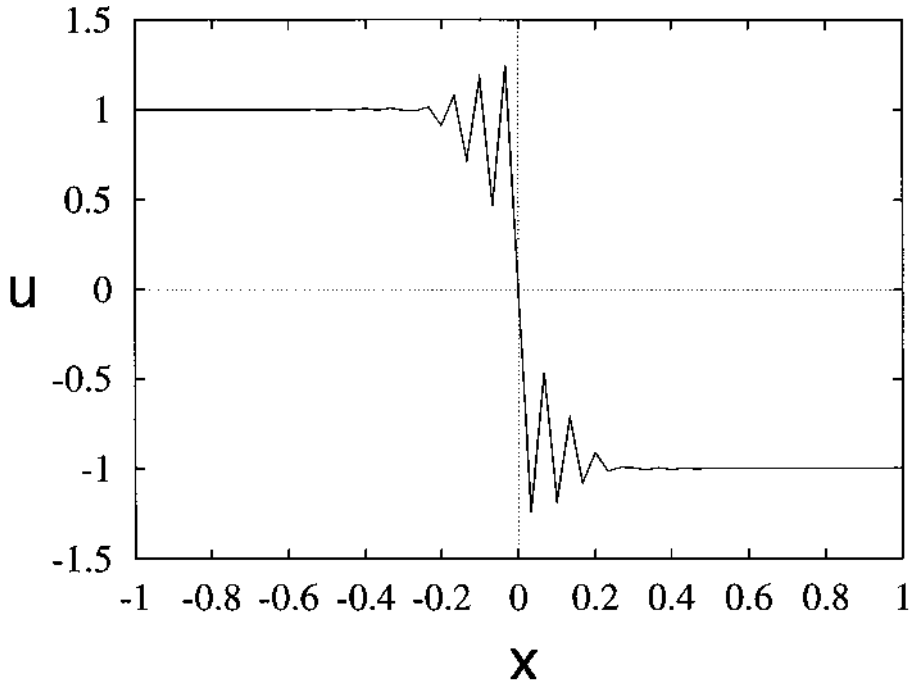

Figure 12.
Problem 3 – Artificial oscillations adjacent to the shock front for ESTSE (uniform mesh; $n_{el} = 30$; $p = 3$)

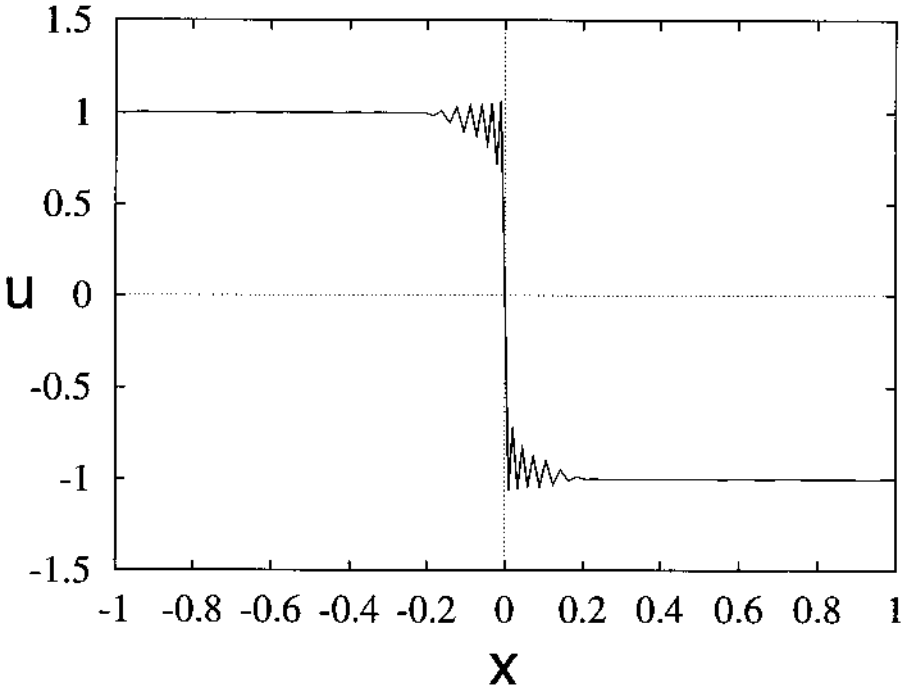

Figure 13.
Problem 3 – Artificial oscillations adjacent to the shock front for STDSE (uniform mesh; $n_{el} = 30$; $p = 3$)

parameters (i.e. for pure convection, pure diffusion and convection-diffusion cases). The potential of this method is greater in convection-dominated problems where severe gradients are encountered.

- A subcycling technique is investigated in the framework of a time-splitting method. Results show that this approach is superior to the others in terms of robustness and CPU time consumption.
- The Burger's equation is the simplest one-dimensional model combining both diffusive and non-linear propagation effects and therefore is classically employed as a test case for numerical algorithms which solve flow problems[1,2,26,28] because its solution can form sharp gradients. Ways to suppress the wiggles at the shock front are investigated. One approach to achieving this objective is to refine the mesh gradually towards the inner boundary layer while using low-order elements in its vicinity. If a uniform mesh is of great importance, it is shown that the wiggles can be suppressed by employing high-order elements in the vicinity of the inner layer and using the natural clustering of the Legendre-Gauss-Lobatto points. This equation is restricted, in the convective sense, to weak shock waves, owing to a lack of pressure gradients. The addition of an inhomogeneous mass source term (as in chemically reactive flows) yields the modified Burger's equation which emulates the influence of an unsteady continuity equation. The result is that the solution can develop strong shock waves. However, these scalar versions of equation (1) are unsatisfactory in both the Cole-Hopf analytic sense (since continuity is not satisfied) and the physical sense (since buoyancy and dissipation are not accounted for). Compressibility effects can be examined via the compressible inviscid one-dimensional Euler equation[7]. However, this is not satisfactory in the physical sense, since it does not account for buoyancy and dissipation effects[29]. In order to account for buoyancy, dissipation and strong shock waves[7], the complete (i.e. vector) two-dimensional (at least) version of equation (1) must be solved. This endeavour is the subject of our current research.
- We can use methods for automatically refining or redistributing spectral element meshes so as to reduce error in the solution[11-13,27,30]. When non-linear problems are considered, adaptive *p*- and *hp*-refinement are very appealing.
- Equations (2) to (3) give a plethora of possibilities for choosing the test and base functions and the refinement strategy[6-8,16,20]. This ability, together with the parallel implementation of the proposed time-splitting method on concurrent processors, makes it very attractive.
- The solution accuracy of convection-dominated problems can be improved through application of the asymptotic spectral element algorithms[22-24].

- Our final goal is to develop space-time spectral elements for solving the full multi-dimensional Navier-Stokes equations. The present paper is another step towards achieving this goal.

References

1. Fletcher, C.A.J., *Computational Techniques for Fluid Dynamics*, Vols I and II, Springer-Verlag, Berlin, 1991.
2. Hirsch, C., *Numerical Computation of Internal and External Flows*, Vol. 1, Wiley, Chichester, 1988.
3. Patera, A.T., "A spectral element method for fluid dynamics: laminar flow in a channel expansion", *Journal of Computational Physics*, Vol. 54, 1984, pp. 468-88.
4. Maday, Y. and Patera, A.T., "Spectral element methods for the incompresssible Navier-Stokes equations", in Noor, A.K. (Ed.), *State of the Art Surveys in Computational Mechanics*, ASME, New York, NY, 1989, pp. 71-143.
5. Maday, Y., Patera, A.T. and Ronquist, E.M., "An operator-integration-factor splitting method for time-dependent problems: application to incompressible fluid flow", *Journal of Scientific Computing*, Vol. 5, 1990, pp. 263-92.
6. Bar-Yoseph, P., "Space-time discontinuous finite element approximations for multi-dimensional non-linear hyperbolic systems", *Computational Mechanics*, Vol. 5, 1989, pp. 145-60.
7. Bar-Yoseph, P. and Elata, D., "An efficient L_2 Galerkin finite element method for multi-dimensional non-linear hyperbolic systems", *International Journal of Numerical Methods in Engineering*, Vol. 29, 1990, pp. 1229-45.
8. Bar-Yoseph, P., Elata, D. and Israeli, M., "An efficient L_2 Galerkin finite element method for multi-dimensional non-linear hyperbolic systems", *International Journal of Numerical Methods in Engineering*, Vol. 36, 1993, pp. 679-94.
9. Bar-Yoseph, P., Moses, E., Zrahia, U. and Yarin, A.L., "Space-time spectral element methods for one-dimensional non-linear advection-diffusion problems", *Journal of Computational Physics*, Vol. 119, 1995, pp. 62-74.
10. Bell, B.C. and Surna, K.S., "A space-time coupled p-version least squares finite element formulation for unsteady fluid dynamics problems", *International Journal of Numerical Methods in Engineering*, Vol. 37, 1994, pp. 3545-69.
11. Demkowicz, L., Oden, J.T., Rachowicz, W. and Hardy, O., "Toward a universal *h-p* adaptive finite element strategy, Part 1. Constrained approximation and data structure", *Computer Methods in Applied Mechanics and Engineering*, Vol. 77, 1989, pp. 79-112.
12. Ewing, R.E. and Lazarov, R.D., "Approximation of parabolic problems on grids locally refined in time and space", *Applied Numerical Mathematics*, Vol. 14, 1994, pp. 199-211.
13. Johnson, C., "Adaptive finite element methods for diffusion and convection problems", *Computer Methods of Applied Mechanical Engineering*, Vol. 82, 1990, pp. 301-22.
14. Johnson, C., Navert, U. and Pitkaranta, J., "Finite element methods for linear hyperbolic problems", *Computer Methods in Applied Mechanics and Engineering*, Vol. 45, 1984, pp. 285-312.
15. Johnson, A.A. and Tezduyar, T.E., "Mesh update strategies in parallel finite element computations of flow problems with moving boundaries and interfaces", *Computer Methods in Applied Mechanics and Engineering*, Vol. 119, 1994, pp. 73-94.
16. Shakib, F., Hughes, T.J.R. and Johan, Z., "A new finite element method for computational fluid dynamics: X. The compressible Euler and Navier-Stokes equations", *Computer Methods in Applied Mechanics and Engineering*, Vol. 89, 1991, pp. 141-219.

17. Weill, A., Shitzer, A. and Bar-Yoseph, P., "Finite element analysis of the temperature field around two adjacent cryo-probes", *ASME, Transactions, Journal of Biomechanical Engineering*, Vol. 115, 1993, pp. 374-9.
18. Zrahia, U. and Bar-Yoseph, P., "Alternative designs towards thermal optimization of coated valves using space-time finite elements", *International Journal of Numerical Methods for Heat and Fluid Flow*, Vol. 4, 1994, pp. 189-206.
19. Zrahia, U. and Bar-Yoseph, P., "Space-time spectral element method for solution of second order hyperbolic equations", *Computer Methods in Applied Mechanics and Engineering*, Vol. 116, 1994, pp. 135-46.
20. Zienkiewicz, O.C. and Taylor, R.L., *The Finite Element Method*, Vol. 2, McGraw-Hill International Editions, London, 1991.
21. Shpitalni, M., Bar-Yoseph, P. and Krimberg, I., "Finite element mesh generation via switching function representation", *Finite Elements in Analysis and Design*, Vol. 5, 1989, pp. 119-30.
22. Bar-Yoseph, P. and Israeli, M., "Asymptotic finite element method for boundary value problems", *International Journal of Numerical Methods in Fluids*, Vol. 6, 1986, pp. 21-34.
23. Bar-Yoseph, P. and Israeli, M., "An asymptotic finite element method for improvement of finite element solutions of boundary layer problems", *Numerische Mathematik*, Vol. 49, 1986, pp. 425-38.
24. Bar-Yoseph, P., Israeli, M. and Weichandler, S., "The asymptotic spectral element method", in Bernardi, C. and Maday, Y. (Eds), *2nd International Conference on Spectral and High Order Methods*, Montpellier, 22-26 June 1992.
25. Celia, M.A. and Gray, W.G., *Numerical Methods for Differential Equations*, Prentice-Hall, Englewood Cliffs, NJ, 1992.
26. Basdevant, C., Deville, M., Haldenwang, P., Lacroix, J.M., Ouazzani, J., Peyret, R., Orlandi, P. and Patera, A.T., "Spectral and finite difference solutions of the Burger's equation", *Computers and Fluids*, Vol. 14, 1986, pp. 23-41.
27. Mavriplis, C., "Adaptive mesh strategies for the spectral element method", *Computer Methods in Applied Mechanics and Engineering*, Vol. 116, 1994, pp. 77-86.
28. Whitham, G.B., *Linear and Non-linear Waves*, Wiley, New York, NY, 1974.
29. Arkadiev, A., Bar-Yoseph, P., Solan, A. and Roesner, K.G., "Thermal effects on axisymmetric vortex breakdown in a spherical gap", *Physics of Fluids*, Vol. A5, 1993, pp. 1211-23.
30. Biswas, R., Devine, K.D. and Flaherty, J.E., "Parallel, adaptive finite element methods for conservation laws", *Applied Numerical Mathematics*, Vol. 14, 1994, pp. 255-83.